JVI Journals.ASM.org

Disulfide Linkages Mediating Nucleocapsid Protein Dimerization Are Not Required for Porcine Arterivirus Infectivity

Rong Zhang, Chunyan Chen, Zhi Sun, Feifei Tan, Jinshan Zhuang, Debin Tian, Guangzhi Tong, and Shishan Yuan

Department of Swine Infectious Diseases, Shanghai Veterinary Research Institute, The Chinese Academy of Agricultural Sciences, Shanghai 200241, China

The nucleocapsid (N) proteins of the North American (type II) and European (type I) genotypes of porcine reproductive and respiratory syndrome virus (PRRSV) share only approximately 60% genetic identity, and the functionality of N in both genotypes, especially its role in virion assembly, is still poorly understood. In this study, we demonstrated that the ORF7 3′ untranslated region or ORF7 of type I is functional in the type II PRRSV background. Based on these results, we postulated that the cysteine at position 90 (Cys90) of the type II N protein, which corresponds to an alanine in the type I protein, is nonessential for virus infectivity. The replacement of Cys90 with alanine confirmed this hypothesis. We then hypothesized that all of the cysteines in the N protein could be replaced by alanines. Mutational analysis revealed that, in contradiction to previously reported findings, the replacement of all of the cysteines, either singly or in combination, did not impair the growth of either type II or type I PRRSV. Treatment with the alkylating agent *N*-ethylmaleimide inhibited cysteine-mediated N dimerization in living cells but not in released virions. Additionally, bimolecular fluorescence complementation assays revealed noncovalent interactions in living cells among the N and C termini and between the N-terminal and C-terminal regions of the N proteins of both genotypes of PRRSV. These results demonstrate that the disulfide linkages mediating the N dimerization are not required for PRRSV viability and help to promote our understanding of the mechanism underlying arterivirus particle assembly.

Porcine reproductive and respiratory syndrome virus (PRRSV) is an enveloped, single-stranded, positive-sense RNA virus belonging to the family *Arteriviridae* in the order *Nidovirales*, which also includes the families *Coronaviridae* and *Roniviridae* (7, 8, 16, 47). Other members of the family *Arteriviridae* include equine arteritis virus (EAV), lactate dehydrogenase-elevating virus (LDV), and simian hemorrhagic fever virus (SHFV) (47). The PRRSV genome is about 15 kb in length, and the coding region is flanked by untranslated regions (UTRs) at each end (the 5′ and 3′UTR, respectively) (36). The genome contains at least 10 open reading frames (ORFs), of which ORF1a and ORF1b encode the two long nonstructural polyproteins pp1a and pp1ab and ORF2 to ORF7 encode at least eight structural proteins, glycoprotein 2 (GP2), small envelope (E), GP3, GP4, GP5, ORF5a, membrane (M), and nucleocapsid (N) (13, 25, 35, 36, 47, 56, 61). The structural proteins are expressed from a set of coterminal subgenomic mRNAs (sgmRNAs), which are synthesized by a unique discontinuous transcription strategy (40). The transcription-regulating sequence (TRS) of the leader (5′UTR) and the downstream body TRS (TRS-B) preceding the ORF coding region of each structural protein in the viral genome are believed to play key roles in mediating this process.

Based on genetic and antigenic differences, PRRSV strains are classified into two distinct genotypes, North American (type II) and European (type I), represented by VR-2332 (4) and Lelystad virus (LV) (53), respectively. It is surprising that these two genotypes, which were identified almost simultaneously as the causative agents of what was then known as blue-ear disease on two different continents, share only approximately 60% nucleotide sequence identity between the overall genomes (1, 14, 18, 34, 39).

The N protein, encoded by ORF7, comprises 123 and 128 amino acids for type II and type I PRRSVs, respectively (47). The N protein is a basic protein and has been shown to be a serine-phosphoprotein (58). It has been detected not only in the cytoplasm but also in the nucleus and nucleolus, and a nuclear localization signal has been identified (42, 43). The N-terminal half of the N protein is presumed to be mostly disordered and involved in RNA binding (12, 62), while the C terminus is believed to be the conformation-determining region of the protein (37, 55, 57). As the sole protein component of the viral nucleocapsid, the N protein has been reported to interact with itself through covalent and noncovalent mechanisms (59). The type II PRRSV N protein contains three conserved cysteine residues at positions 23, 75, and 90; cysteine 23 (Cys23) is capable of forming N-N disulfide linkages (59). Cysteine-to-serine mutational analysis using an infectious cDNA clone confirmed this property and also revealed that the cysteine at position 90 (Cys90) is essential for virus infectivity (31). This raised the question of how the type I N protein is able to function despite having no cysteine corresponding to the type II N Cys90. Indeed, the cysteine residue number patterns in N protein are highly divergent among the different arterivirus family members. There are only two cysteines in the N protein of the type I PRRSV and LDV, and there are none in EAV or SHFV (10, 15, 28, 36).

The N protein is critical for genome encapsidation and virion assembly. Although the crystal structure of a partial N protein from type II PRRSV has been determined (11), the exact structure-function relationship is still poorly understood. Knowing that the N proteins of the two PRRSV genotypes are genetically and antigenically diversified, we explored the possibility of engineering chimeric PRRSVs containing heterologous ORF7 (N gene) and/or 3′UTR sequences, presuming that such constructs

Received 4 November 2011 **Accepted** 20 January 2012
Published ahead of print 1 February 2012
Address correspondence to Shishan Yuan, shishanyuan@hotmail.com.

doi:10.1128/JVI.06709-11

could be helpful to dissect the functionality of the N protein and elucidate the mechanism of virion assembly. Here, we demonstrate that the distantly related N protein of a type I virus is functional in the genetic background of a type II PRRSV. Site-directed mutagenesis demonstrated that all of the N protein cysteines are nonessential for virus infectivity for both genotypes of PRRSV. Although the disulfide-linked N dimers still were present in mature virions, our results reveal that the cysteine-mediated N-N disulfide linkage is not required for porcine arterivirus viability in cultured cells.

MATERIALS AND METHODS

Cells, plasmids, and reagents. MARC-145 cells were cultured as described in our previous study (49). The infectious cDNA clone pAPRRS (GenBank accession no. GQ330474) was derived from the type II PRRSV strain APRRS (63). The infectious cDNA clone pSHE (GQ461593) was derived from the type I strain SHE (49). These two clones were modified to be driven by the eukaryotic cytomegalovirus (CMV) promoter as previously described (31). The mammalian expression vector pCAGGS was kindly provided by Zejun Li (Shanghai Veterinary Research Institute, China). Cell lysis buffer for Western blotting and immunoprecipitation containing 1 mM phenylmethylsulfonyl fluoride (PMSF) (referred to here as lysis buffer) was purchased from the Beyotime Institute of Biotechnology (China). The sulfhydryl-reactive reagent *N*-ethylmaleimide (NEM) and the reducing agent dithiothreitol (DTT) were purchased from Sigma-Aldrich.

Plasmid construction. The splicing overlap extension PCR strategy (19) was employed to construct the chimeric clones, as shown in Fig. 1A. The intermediate PCR products were amplified using pAPRRS and pSHE as templates, and the resulting two segments were spliced in a subsequent PCR. The final product and parental pAPRRS were digested with SpeI/XhoI (New England BioLabs) and then ligated by T4 DNA ligase to construct the full-length chimeric clones pA-SHE73′ and pA-OSHE73′. The 3′UTR of pA-OSHE73′ then was replaced with the counterpart from pA-PRRS to generate the pA-OSHE7 clone using the same PCR strategy. For site-directed mutagenesis, two shuttle plasmids, pTB5c (63) and pSHEex, were used. Plasmid pSHEex was generated by insertion of the 3′ terminus of the SHE genome into pBluescript II SK(+) with EcoRI and XbaI. Mutagenic PCR was performed to replace the cysteine codon (TGC) in the N protein with an alanine (GCG) or serine (AGC) codon. The SpeI/XhoI and EcoRI/XbaI fragments carrying the cysteine mutations were obtained from the shuttle plasmids and subcloned into the full-length cDNA clone pAPRRS or pSHE to replace the respective corresponding segments. These new mutants were named as shown in Fig. 2B. For the expression of N protein by a mammalian vector, the full-length N gene was amplified from pAPRRS or pSHE and cloned into pCAGGS with EcoRI and XhoI, resulting in the pCAGG-AN and pCAGG-SN constructs. pCAGG-AN-C23A and pCAGG-SN-C27A were generated from the clones pAN-C23A and pSN-C27A (Fig. 2B), respectively, in the same manner. All of the chimeric and mutant clones were verified by the restriction enzyme digestion pattern of the plasmid and nucleotide sequencing of the PCR-manipulated region. All of the primers used for plasmid construction are available upon request.

DNA transfection. The infectious cDNA clones pAPRRS, pSHE, and their derivatives were isolated using the QIAprep spin miniprep kit (Qiagen). MARC-145 cells at approximately 80% confluence in 6-well plates were transfected with 2 μg/well DNA prepared using the FuGENE HD transfection reagent (Roche) according to the manufacturer's protocol. When about 80% cytopathic effect (CPE) was observed, the cell culture supernatants were collected and designated passage 1 (P1). The P1 viruses were used to inoculate fresh MARC-145 cells, and the P2-P3 virus stocks were prepared in the same manner. For N protein expression by pCAGGS, the plasmids were transfected by the strategy described above. At 36 h posttransfection, the cells were subjected to SDS-PAGE and Western blotting.

RT-PCR and nucleotide sequencing. Viral genomic RNA was isolated using a QIAprep viral RNA minikit (Qiagen), and total intracellular RNA was isolated using TRIzol reagent (Invitrogen) according to the manufacturer's instructions. To verify the chimeric and mutant viruses, reverse transcription-PCR (RT-PCR) was performed with avian myeloblastosis virus reverse transcriptase (TaKaRa, China) and *Pfu*Ultra II Fusion HS DNA polymerase (Stratagene). The PCR products were gel purified and subjected to nucleotide sequencing. All of the primers used for sequencing are available upon request.

Northern blot analysis. Total cellular RNA was isolated from MARC-145 cells at day 2 posttransfection as described above. Northern blotting was performed with the NorthernMax kit (Ambion) by following the manufacturer's instructions. Total RNA was loaded at 10 μg per lane and separated by electrophoresis on 1% formaldehyde-denatured agarose gels and then transferred to a BrightStar-Plus membrane (Ambion) and cross-linked with UV light. Samples were probed with a biotin-labeled oligonucleotide that specifically recognizes the type I PRRSV ORF7 (EU-ORF7; 5′-GGCCTGTCCTCCCCTAGGTTGCTGGCGCTGGGACTTTATCATTGC-3′).

After hybridization overnight at 42°C, the filters were incubated with alkaline phosphatase-conjugated streptavidin followed by the chemiluminescent substrate CDP-STAR detection reagent (Ambion). Immunoreactive bands were visualized by exposure to Kodak film.

IFA. At day 2 posttransfection, indirect immunofluorescence analysis (IFA) was performed on the MARC-145 cell monolayers as described previously (49). Briefly, cells were fixed with cold methanol followed by blocking with 1% bovine serum albumin (BSA) and then incubated for 2 h with a monoclonal antibody (MAb) (1AG11) that specifically recognizes both type II and type I PRRSV N proteins (kindly provided by Ingenasa Co., Madrid, Spain). After washing with phosphate-buffered saline (PBS), the cells were incubated for 1 h with Alexa Fluor 568-labeled goat anti-mouse secondary antibody (Invitrogen). After a final PBS wash step, cells were visually analyzed by using an Olympus inverted fluorescence microscope.

Viral plaque and growth kinetics assays. The viral plaque and growth kinetics assays were conducted as previously described, with minor modifications (49). For the plaque assays, the rescued P1 viruses were diluted serially and used to infect MARC-145 cells cultured in 6-well plates. After incubation, the cells were washed and overlaid with modified Eagle's medium (2× MEM; Invitrogen) containing 4% fetal bovine serum (FBS) and mixed with an equal volume of 2% low-melting-point agarose (Cambrex). After 3 to 5 days of incubation at 37°C, the plaques were stained with crystal violet. To determine the growth curves, the MARC-145 cells were infected with P1 viruses at a multiplicity of infection (MOI) of 0.1. After incubation, the cells were washed and cultured with Eagle's minimal essential medium (EMEM; Invitrogen) supplemented with FBS. The culture supernatants (200 μl/well) were collected at 6, 12, 24, 36, 48, 60, 72, 96, and 108 h postinfection, and the progeny virus titers were determined by 50% tissue culture infectious doses ($TCID_{50}$/ml).

Purification of extracellular virions. MARC-145 cells in 100-mm dishes were infected with each parental or mutant virus at various multiplicities of infection. At about 24 h postinfection, before any CPE was observed, cell supernatants (200 ml) containing virions were subjected to centrifugation at 6,000 × *g* at 4°C for 30 min in a Beckman JA-10 rotor to remove cellular debris. Virions in the supernatants were pelleted through a 30% sucrose cushion in a buffer containing 50 mM HEPES, 100 mM NaCl, and 1 mM EDTA, pH 7.2, by ultracentrifugation at 110,000 × *g* at 4°C for 3 h in an SW32 Ti rotor. The pellets were resuspended in a buffer containing 50 mM HEPES, 100 mM NaCl, and 1 mM EDTA, pH 7.2, and again pelleted by centrifugation through the same cushion under the same conditions but with an SW41 rotor. The final pellets were resuspended in lysis buffer and subjected to SDS-PAGE and Western blotting. For the isolation of NEM-treated virions, the cell supernatants were prepared as described above and incubated with NEM (final concentration, 5 mM) for 30 min at room temperature. NEM (5 mM) was also used during all

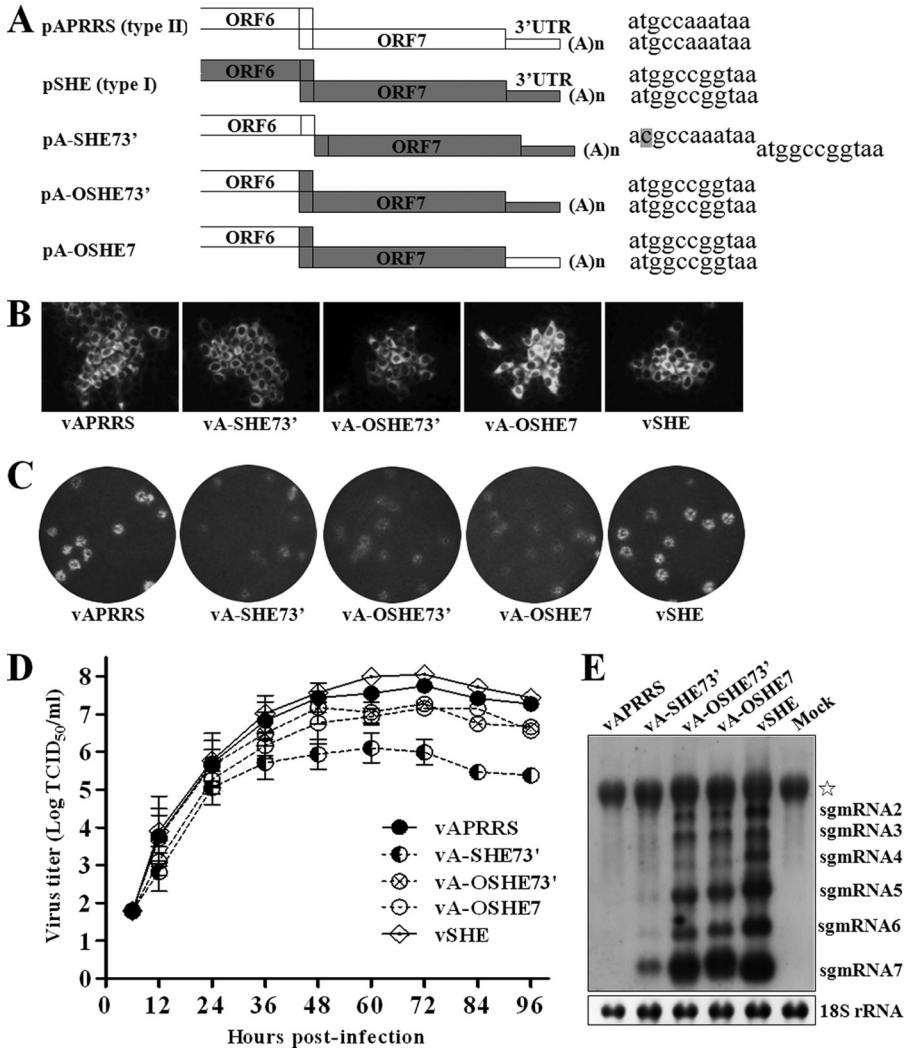

FIG 1 Type I N protein can function in the type II PRRSV background. (A) Schematic diagram of the chimeras. The infectious cDNA clones of the type II PRRSV strain APRRS and the type I strain SHE are indicated as white and gray boxes, respectively. The sequences after the boxes show the junction of ORF6 and ORF7. Chimeric constructs were generated as detailed in Materials and Methods. For pA-SHE73′, the ORF7 3′UTR segment of SHE was placed immediately downstream of ORF6 of APRRS, the overlap between ORF6 and ORF7 was separated, and the start codon AUG for the type II ORF7 in the duplication of the overlap was mutated to ACG. For pA-OSHE73′, the overlap between ORF6 and ORF7 was maintained as in SHE, and pA-OSHE7 was derived from pA-OSHE73′ by replacing the 3′UTR with its counterpart from APRRS. (B) Indirect immunofluorescence analysis was conducted to verify heterologous N protein expression. Two days after transfection, MARC-145 cells were fixed and stained with a MAb that can specifically recognize both genotypes of PRRSV N protein, further incubated with an Alexa Fluor 568-labeled goat anti-mouse antibody, and then visualized by inverted fluorescence microscopy. (C) Plaque morphology. The P1 viruses were used to inoculate MARC-145 cells for 1 h, overlaid with 1% agarose, and incubated for about 4 days until plaques developed. Plaques were stained with 1% crystal violet. (D) Growth kinetics. MARC-145 cells were infected with P1 chimeric viruses at an MOI of 0.1, and the supernatants were harvested at the indicated time points. Virus titer was determined by the $TCID_{50}$/ml, and the results are presented as mean values from three independent experiments. (E) The subgenomic RNA transcription profiles were analyzed by Northern blotting. Two days after the transfection of MARC-145 cells, RNAs from each sample were loaded and separated by 1% agarose gel electrophoresis and then transferred to the membrane. sgmRNAs were hybridized with a type I-specific PRRSV probe located in ORF7. 18S rRNA was used as an internal control. The nonspecific band is indicated by an asterisk.

subsequent steps (performed as described above). An additional alternative purification method was also employed. Briefly, cell supernatants (1 liter) were prepared and subjected to CsCl density gradient centrifugation as previously described (25). The purified virus band was removed with a sterile needle and incubated with 5 mM NEM for 30 min at room temperature before being subjected to SDS-PAGE and Western blotting.

SDS-PAGE and Western blotting. PRRSV-infected or pCAGGS expression vector-transfected cells in 6-well plates were washed twice with PBS and lysed with lysis buffer in the presence or absence of 1 mM NEM. After incubation for 10 min at room temperature, cell lysates were centrifuged at 12,000 × *g* for 5 min and the supernatants collected. Protein samples were prepared in reducing buffer (50 mM Tris, pH 6.8, 10% glycerol, 2% SDS, 0.02% [wt/vol] bromophenol blue, 100 mM DTT) or nonreducing buffer (50 mM Tris, pH 6.8, 10% glycerol, 2% SDS, 0.02% [wt/vol] bromophenol blue). Samples then were heated at 95°C for 5 min, resolved on 12% SDS polyacrylamide gels, and transferred to Hybond-P membranes (Amersham Biosciences). Membranes were blocked with 5% nonfat dry milk in TBST (100 mM NaCl, 10 mM Tris, pH 7.6, 0.1% Tween 20) for 2 h at room temperature. Membranes were incubated overnight at 4°C with primary antibody (1AG11) specific to both type II and type I PRRSV N proteins. After washing with TBST, blots were incubated with horseradish peroxidase (HRP)-conjugated goat anti-mouse secondary

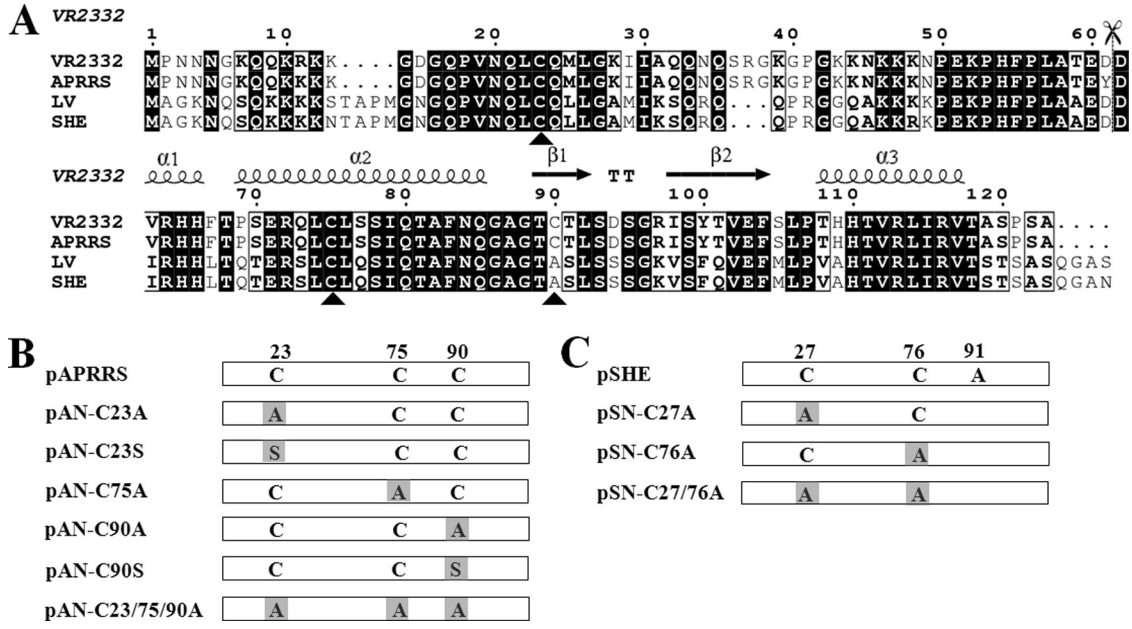

FIG 2 Sequence alignment of PRRSV N proteins and the construction of cysteine mutants. (A) Alignment of N sequences from type II PRRSV strains (VR2332, GenBank accession no. U87392; APRRS, GQ330474) with the corresponding sequences from type I strains (LV, M96262; SHE, GQ461593). Completely conserved residues are indicated in black boxes, and partially conserved residues are in white boxes. The cysteines at positions 23, 75, and 90 of the type II N protein are indicated by black triangles. The scissors indicate the split site of the N protein for the BiFC assay. The secondary structure elements above the sequence show the structure of the C terminus of the VR2332 N protein (11). This figure was generated by ESPript (17), with slight modifications. (B) The cysteine residues in the N protein of APRRS and SHE were replaced with alanine or serine, either alone or in combination. The number above the boxes indicates the location of the cysteine or alanine. PCR-based site-directed mutagenesis was used to replace the codon for cysteine (TGC) with that of alanine (GCG) or serine (AGC).

antibody (Santa Cruz) for 1 h at room temperature, washed again with TBST, and developed using SuperSignal West Pico or Femto chemiluminescent substrate according to the manufacturer's instructions (Thermo Fisher Scientific).

BiFC assay. A variant of yellow fluorescent protein, Venus, was obtained by the site-directed mutagenesis of pEYFP-N1 (BD-Clontech) as previously described (38). As shown in Fig. 7A, sequences encoding the amino (residues 1 to 173; VN) or carboxyl (residues 174 to 239; VC) fragment of Venus were fused to the C terminus of the full-length or truncated N proteins via a $(GGGGS)_3$ linker (44, 46). We also amplified the alpha-tubulin gene from MARC-145 cell lines to be fused to the N termini of VN and VC for use as negative controls. Detailed sequence information for each construct is available upon request. MARC-145 cells cultured in 6-well plates to about 60% confluence were cotransfected with 500 ng of each bimolecular fluorescence complementation (BiFC) plasmid using the FuGENE HD transfection reagent. At 16 h posttransfection, live cells were visualized using an Olympus inverted fluorescence microscope.

RESULTS

Type I N protein is functional in the type II PRRSV background. The nucleotide and predicted amino acid sequences of the N protein are extremely conserved within each genotype but show only about 60% identity between genotypes (Fig. 2A). Our previous work had demonstrated that the envelope structural proteins (ORF2 to ORF5) of type I PRRSV are fully functional in the type II PRRSV background (49). To investigate whether the N protein is exchangeable between type II and type I PRRSV, reverse genetic manipulation was conducted based on the infectious cDNA clones of pAPRRS and pSHE (Fig. 1A), which represent the type II and type I PRRSV genotypes, respectively. The overlapping coding sequences shared by the adjacent ORF6 and ORF7 pose a problem for the construction of chimeric PRRSV. To overcome this challenge, we rearranged ORF6 and ORF7 and engineered three chimeric clones: pA-SHE73′, pA-OSHE73′, and pA-OSHE7 (shown schematically in Fig. 1A). pA-SHE73′ contained the ORF7 3′UTR of SHE; the overlap between ORF6 and ORF7 was separated without any intervening inserted sequence, and the extra AUG for type II ORF7 was knocked out to prevent the frameshifting from occurring during the N translation by forcing the chimeric virus to utilize the authentic AUG for type I ORF7. For pA-OSHE73′, the overlap between ORF6 and ORF7 was maintained as in SHE, changing two amino acids in the C terminus of the M protein of APRRS. As for pA-OSHE7, ORF7 of SHE was forced to replace its counterpart in APRRS in an exact ORF-for-ORF substitution. These chimeras and their parental clones (pAPRRS and pSHE) were transfected into MARC-145 cells, which were then observed for cytopathic effect (CPE). At about 3 days posttransfection, the chimeric plasmids produced visible CPE (data not shown) similar to that induced by the parental clones. An indirect immunofluorescence assay was then conducted, and it indicated that the N protein of SHE can be expressed in the background of APRRS. The clusters of stained cells shown in Fig. 1B indicate the spread of virus infection.

To assess the virological properties of the chimeric viruses, the rescued P1 viruses were used to infect fresh MARC-145 cells and viral plaque assays were performed. There was no distinguishable difference in plaque morphology among vA-SHE73′, vA-OSHE73′, and vA-OSHE7. The chimeric plaques were slightly reduced in size and sometimes poorly visible compared to the

wild-type plaques (Fig. 1C). The cells in the centers of the plaques died more readily and detached earlier for the parental viruses (vAPRRS and vSHE), while the centers of the chimeric plaques contained more viable cells, which possibly contributed to the obscured plaque phenotype. The growth kinetics of the P1 viruses also were evaluated. As shown in Fig. 1D, the growth patterns of vA-OSHE73′ and vA-OSHE7 appeared to be similar to those of the parental vAPRRS and vSHE, albeit with peak titers 0.5 log lower than those of the parental viruses. It is noteworthy that the vA-SHE73′ titer was consistently lower than that of the other viruses, especially from 36 h postinfection, and the peak titer was two logs lower than that of the parental viruses. We then analyzed the subgenomic RNA profiles to assess the effect of chimeric manipulation on virus transcription. Northern blotting was conducted on MARC-145 cells 2 days posttransfection using a synthetic biotin-labeled probe that can detect the chimeras and the type I vSHE but not the type II vAPRRS. As shown in Fig. 1E, the levels of sgmRNAs, like sgmRNA4 and sgmRNA6, were proportionately and strongly reduced in vA-OSHE73′ and vA-OSHE7 compared to those of the parental vSHE. However, vA-SHE73′ displayed much lower levels of sgmRNAs.

Nucleotide sequencing of the ORF7 3′UTR region then was performed for the P1 and P3 chimeric viruses. No nucleotide mutation was found in vA-OSHE73′ or vA-OSHE7, but the P1 and P3 vA-SHE73′ sequences had a single-amino-acid mutation in the N protein (K11R; codon AAG to AGG). We also chose passage 3 of vA-OSHE7 for full-length genomic sequencing and found that it contained only two silent mutations, one at nucleotide 7920 (A to G) in the predicted nsp9 coding region and the other at 13769 (C to T) in ORF4, indicating that the chimeric viruses can remain generally stable for at least three passages in cultured cells. These findings demonstrated for the first time that the type I N protein is functional in the backbone of type II PRRSV despite the low similarity of the N proteins between the genotypes.

All of the cysteines in the N protein are nonessential for type II and type I PRRSV viability. Since the N gene of type II PRRSV could be replaced by its type I counterpart, we speculated that the intergenotypically conserved domains or amino acids play a more significant role in N functionality. The N protein sequence alignment revealed that SHE and all type I PRRSV sequences contain an alanine residue corresponding to position 90 of the N protein of type II viruses, such as APRRS (Fig. 2A). A previous study revealed that the replacement of cysteine with serine at position 90 in type II is lethal for virus infectivity (31). Based on our chimera study, we hypothesized that Cys90 of the type II N protein could be successfully replaced by alanine. We constructed the mutant pAN-C90A in which the Cys90 codon (TGC) of the APRRS N gene was mutated to an alanine codon (GCG) (Fig. 2B). As a control, we also constructed another cysteine mutant, pAN-C90S, in which Cys90 was replaced with serine (AGC), as previously reported (31). The mutants were transfected into MARC-145 cells, which were monitored daily for the appearance of CPE. Surprisingly, both the pAN-C90A mutant and the parental pAPRRS produced visible CPE about 3 days posttransfection (data not shown). In contrast, pAN-C90S did not induce any visible CPE even after prolonged incubation for up to 7 days. To further confirm this result, we have (i) repeated the nucleotide sequencing of the full-length pAN-C90S clone, (ii) repeated the transfection at least three times, (iii) blindly passaged the transfection supernatant for CPE observation, and (iv) detected the viral RNA by RT-PCR. However, these measures failed to verify the production of infectious progeny of pAN-C90S (data not shown), which is in agreement with previous reports (31). We then further hypothesized that all of the cysteine residues of the N protein could be replaced by alanine. To test this, three mutants were constructed, pAN-C23A, pAN-C75A, and pAN-C23/75/90A, in which the single cysteines at positions 23 and 75 or all three of the cysteines in the type II N protein, respectively, were mutated to alanine (Fig. 2B). As expected, all of these mutants could produce infectious viruses when transfected into MARC-145 cells. Notably, another mutant, pAN-C23S (Cys23 to serine), that was previously reported to be lethal (31), could also induce CPE (data not shown). The nucleotide changes made in the pAN-C90S and pAN-C23S mutants were identical to those in the previous study (31). The expression of N proteins was confirmed by IFA, as shown in Fig. 3A. The staining of single cells for pAN-C90S revealed that there were no infectious progeny released.

We then characterized the virological properties of the mutant viruses. Plaque morphology and growth kinetics were indistinguishable among vAN-C23A, vAN-C75A, vAN-C90A, and parental vAPRRS, while vAN-C23/75/90A showed somewhat smaller plaque size and a peak titer 0.5 log lower than that of the parental virus (Fig. 3B and C). The pinpoint plaque size and much lower growth rate of vAN-C23S revealed that the mutation greatly affected viral replication (Fig. 3B).

To further verify these findings, we engineered similar mutations in the type I PRRSV background, represented in our study by SHE. The cysteines at positions 27 (Cys27) and 76 of the N protein were mutated to alanine either alone or in combination (as illustrated in Fig. 2C). When transfected into cells, all of these mutants could induce CPE (data not shown), and IFA demonstrated their corresponding expression of N proteins (Fig. 4A). The rescued viruses showed no significant differences in plaque size or growth rate compared to those of the parental vSHE (Fig. 4B and C).

To assess their genetic stabilities, all of these cysteine mutants of both type II and type I PRRSV were passaged three times on MARC-145 cells, and the ORF7 regions from both the P1 and P3 viruses were sequenced. The sequencing data showed that all of the engineered cysteine mutations were retained for at least three passages. No second-site mutation was found in these viruses, with the exception of a single-amino-acid change (E71V; codon GAG to GTG) in the P1 and P3 vAN-C23S sequences. These results demonstrated that, in contrast to what was previously believed (31), all of the N protein cysteine residues are nonessential for type II and type I PRRSV infectivity.

NEM treatment prevents disulfide-linked N dimerization in cells but not in extracellular virions. The facts that both genotypes of PRRSV remained viable after all N protein cysteines were mutated and that their virological properties were similar to those of the parental viruses contradicted previously published findings from others, which showed that Cys23 and Cys90 were essential for type II PRRSV infectivity and that Cys23-mediated disulfide bond formation was involved in N protein homodimerization (31, 59). Thus, we attempted to explore the biochemical evidence of disulfide bond formation in both intracellular N proteins and extracellular virions. First, we investigated whether disulfide bond formation is involved in N protein homodimerization in PRRSV-infected cells. MARC-145 cells were infected with all of the mutant and parental viruses. About 24 h postinfection, before any CPE was observed, cells were harvested in lysis buffer in the presence or

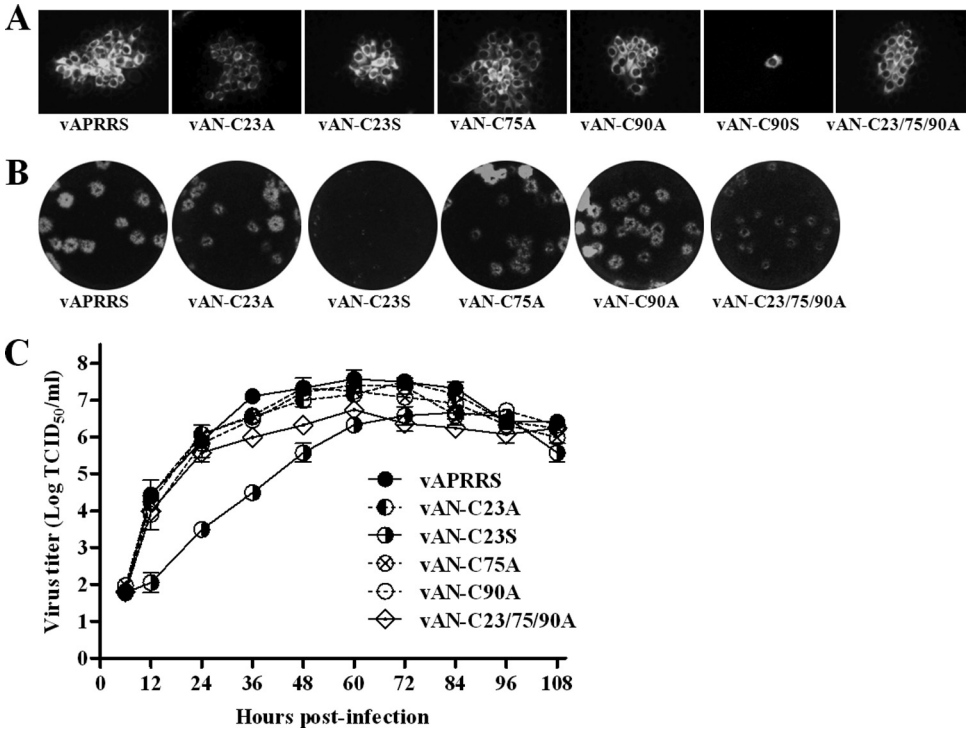

FIG 3 All of the type II N protein cysteines can be knocked out without effect. (A) IFA showing the expression of N protein. The clusters of stained cells represent the spread of virus infection, whereas the single cell indicates the absence of released live virus. (B) Plaque morphology of cysteine mutants. (C) Growth kinetics were examined, and the results are presented as mean values from three independent experiments.

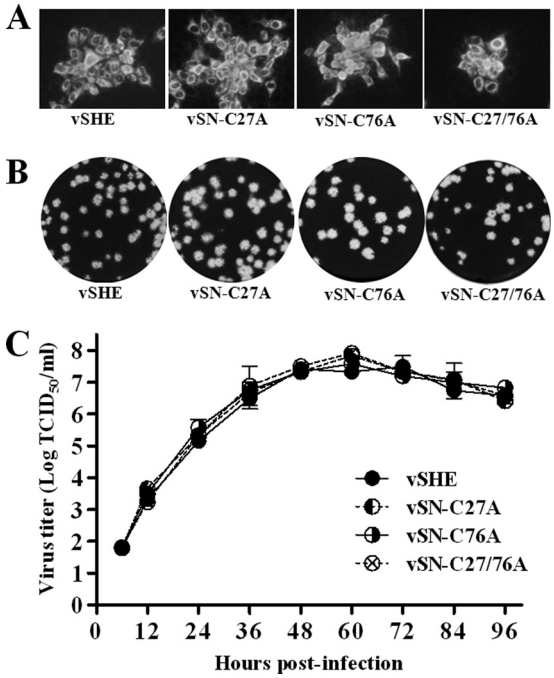

FIG 4 Cysteine knockout mutants of type I PRRSV show virological properties similar to those of the parental virus. (A) Expression of N protein was verified by IFA. (B) Plaque morphology. (C) Growth curves for cysteine mutants and the wild-type virus. The results are presented as mean values from three independent experiments.

absence of 1 mM NEM. The alkylating agent NEM is a small membrane-permeable compound that can irreversibly modify the free thiols of cysteine residues, thereby preventing *de novo* disulfide bond formation. Cell lysates were resolved by SDS-PAGE under reducing and nonreducing conditions and subjected to Western blotting. The results showed that in the absence of both the reducing agent DTT and the alkylating agent NEM, N proteins expressed from vAPRRS, vAN-75A, vAN-90A, vSHE, and vSN-76A formed dimers as well as monomers (Fig. 5A and B), whereas those from vAN-23A, vAN-23/75/90A, vSN-27A, and vSN-27/76A produced only monomers. To distinguish between disulfides preformed in cells and those formed only after cell lysis, NEM was included in the lysis buffer to block new disulfide bond formation. Under nonreducing conditions in the presence of NEM, we could not detect N protein dimerization for any of the type II or type I parental or mutant viruses (Fig. 5A and B). In addition, the same phenomena occurred when N proteins with (Cys23 to A and Cys27 to A for the type II APRRS and type I SHE N proteins, respectively) or without the cysteine mutations were expressed from the mammalian vector pCAGGS (Fig. 5C). These results demonstrated that Cys23 in type II and Cys27 in type I PRRSV participated in disulfide-linked N protein homodimerization that could be prevented by lysing cells in the presence of NEM, suggesting that the disulfide bond formation observed had occurred when the N proteins were exposed to the oxidizing extracellular environment after cell lysis.

To further confirm that the formation of cysteine-mediated disulfide bonds in cytoplasmic N dimers was aberrant and occurred only after cell lysis, virus-infected or pCAGGS-transfected cells were incubated at 37°C in EMEM containing 1 mM NEM for

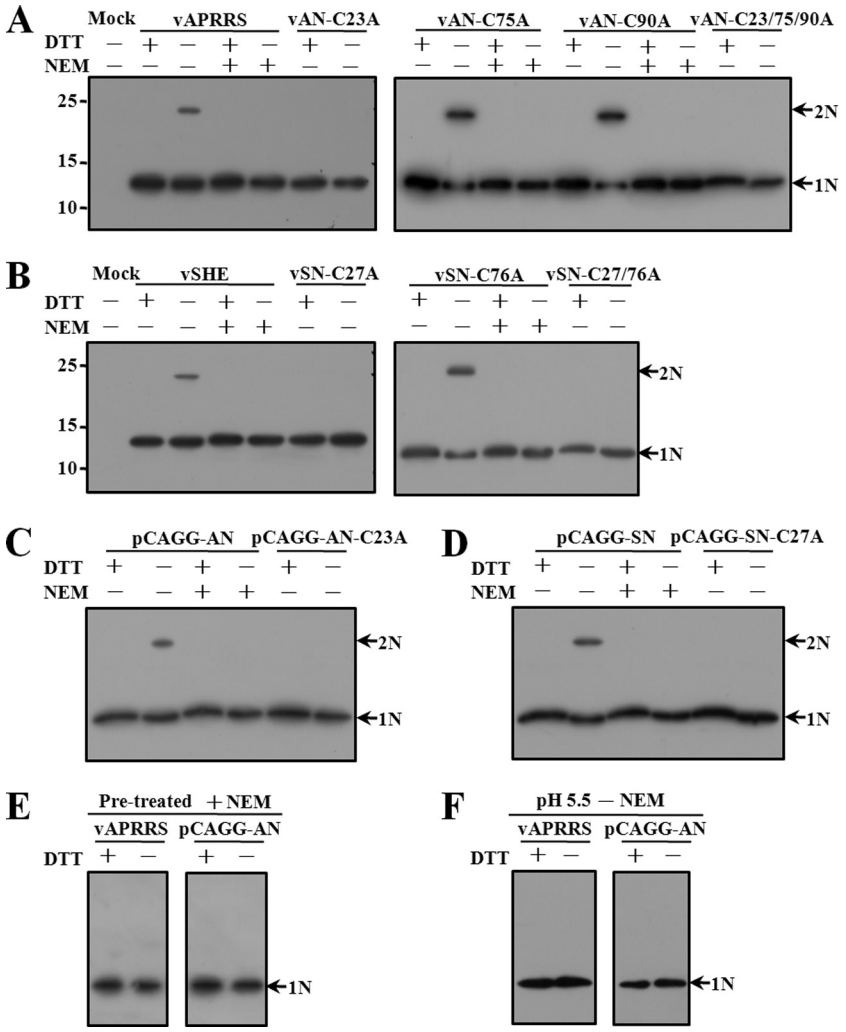

FIG 5 Dimerization of cellular N proteins. Virus-infected or expression vector pCAGGS-transfected cells were lysed in the presence (+) or absence (−) of 1 mM NEM, separated by SDS-PAGE under reducing (+DTT) or nonreducing (−DTT) conditions, and subjected to Western blot analysis. (A) N proteins expressed from wild-type and mutant type II PRRSV APRRS. (B) N proteins expressed from wild-type and mutant type I PRRSV SHE. (C) Wild-type and cysteine mutant APRRS N proteins expressed from the mammalian vector pCAGGS. (D) Wild-type and cysteine mutant SHE N proteins expressed from pCAGGS. (E) Cellular APRRS N proteins expressed from virus or pCAGGS were treated with 1 mM NEM before cell lysis. Cells then were lysed without NEM and subjected to SDS-PAGE under reducing or nonreducing conditions, followed by Western blotting. (F) Cellular APRRS N proteins expressed from virus or pCAGGS were lysed at pH 5.5 without NEM treatment. Cell lysates then were subjected to SDS-PAGE under reducing or nonreducing conditions and analyzed by Western blotting. Monomers (N) or dimers (2N) of the N protein are indicated by arrows.

10 min prior to harvesting, which ensured that any disulfide bonds detected in cells had, in fact, formed in cells prior to lysis, and then they were harvested in lysis buffer without additional NEM. As shown in Fig. 5E, only N protein monomers were detected under these conditions. As an alternative method, cells were harvested in NEM-free lysis buffer at pH 5.5; such low pH is expected to prevent disulfide bond formation. SDS-PAGE under nonreducing conditions and Western blot analysis demonstrated that the disulfide linkage of N-N interactions was blocked (Fig. 5F). Taken together, these observations suggest that the N protein cysteines have an intrinsic ability to form disulfide bonds, but only under oxidizing conditions.

We next investigated whether the disulfide bonds between N proteins could be detected in extracellular virions. Virions in the supernatants were pelleted twice through a 30% sucrose cushion, as described in Materials and Methods, and then analyzed by SDS-PAGE under reducing and nonreducing conditions followed by Western blotting. When Cys23 in the APRRS N protein or Cys27 in the SHE protein was not mutated to alanine, the disulfide-linked N dimers were found to be present in the extracellular virus particles collected in the absence of NEM under nonreducing conditions (Fig. 6A and B), as detected with samples of cellular N proteins. However, as shown in Fig. 6C, NEM treatment did not prevent the dimerization of the N proteins of either vAPRRS or vSHE virions collected under nonreducing conditions. Both the monomeric and dimeric N proteins were detectable for both vAPRRS and vSHE particles, regardless of whether NEM was present throughout the purification process or only in the lysis buffer in the last resuspension step, or even when its concentration was increased to 20 mM (data not shown). Furthermore, to obtain highly purified virus particles, we performed CsCl equilibrium density gradient centrifugation on supernatants containing

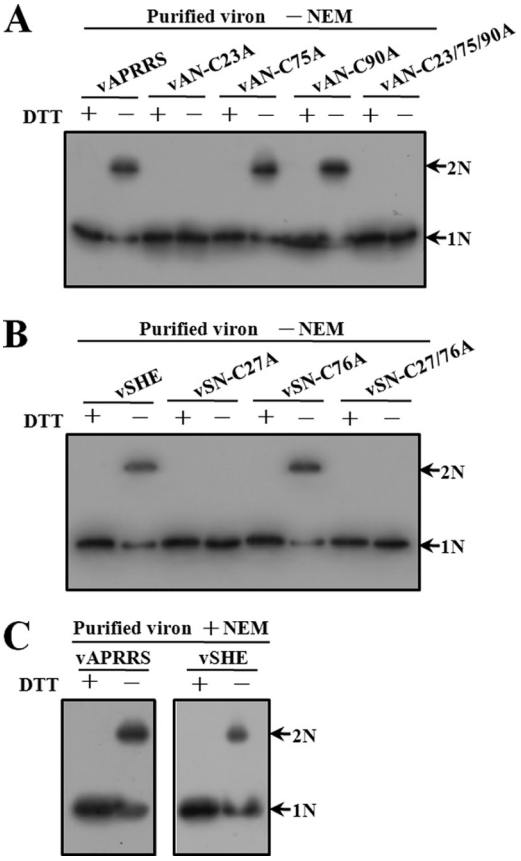

FIG 6 Dimerization of N proteins in extracellular virions. Virions from culture supernatants were purified in the absence or presence of NEM as described in Materials and Methods. Purified particles were resolved by SDS-PAGE under reducing or nonreducing conditions and subjected to Western blot analysis. (A) Purified wild-type and mutant APRRS particles without NEM treatment. (B) Purified wild-type and mutant SHE particles without NEM treatment. (C) Purified APRRS and SHE particles with NEM treatment. Monomers (N) or dimers (2N) of the N protein are indicated by arrows.

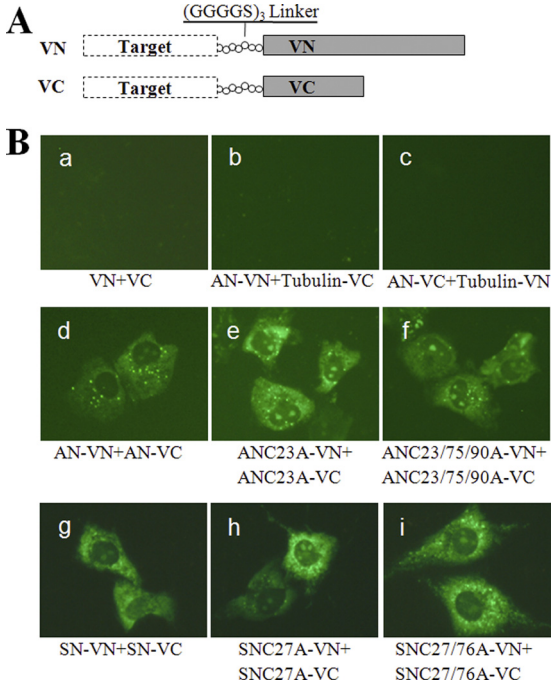

FIG 7 BiFC analysis of full-length N proteins. (A) Schematic diagram of BiFC constructs. The Venus protein was split between amino acid residues 173 and 174, resulting in fragments VN (N-terminal 173 residues) and VC (C-terminal 66 residues). The so-called Target protein was fused to the N terminus of VN or VC with a linker sequence to generate the BiFC pair. (B) Visualization of interactions between full-length N proteins in living cells. Fragments VN and VC or α-tubulin gene-fused VN and VC were coexpressed in MARC-145 cells, and the fluorescent signals were examined as negative controls to assess the specificity of the BiFC method (panels a to c). Full-length N proteins from both genotypes of PRRSV with or without cysteine mutations were fused to the N terminus of VN or VC, and cells were cotransfected and examined for fluorescence (panels d to i).

vAPRRS virions, and disulfide-linked N dimers were still detected in the presence of NEM (data not shown). Collectively, these results confirmed that the disulfide-linked N dimerization occurs in the mature virions and is mediated by C23 in type II or C27 in type I N, which is in line with a previous study (59).

***In vivo* characterization of N-N interactions by BiFC.** Previous reports have demonstrated that not only the cysteine-mediated covalent interactions but also noncovalent interactions are involved in N protein dimerization (59). To better understand the status of N dimerization, we employed a newly developed technique, known as bimolecular fluorescence complementation (BiFC). The BiFC assay was first developed by Hu and colleagues (21) for investigating protein-protein interactions, and it is a powerful tool to specifically and sensitively detect weak or otherwise-transient protein-protein interactions *in vivo* (22, 27, 45). BiFC is based on the principle that two interacting proteins individually fused to the N- and C-terminal fragments of a fluorescent protein can bring the two halves of the fluorescent protein into close proximity, thereby facilitating the reconstitution of the fluorophore. As such, BiFC assays allow for the visualization and localization of specific protein-protein interactions within living cells.

We used Venus, a variant of enhanced yellow fluorescent protein, for the BiFC assays in our study. We first split the fluorescent protein between amino acid residues 173 and 174 to generate two fragments, VN and VC. As expected, neither VN nor VC alone produced a fluorescent signal when expressed in MARC-145 cells (data not shown). Likewise, the coexpression of VN and VC produced no fluorescence (Fig. 7B, panel a). We then generated chimeric constructs in which the full-length N protein of APRRS was fused to the N terminus of VN or VC with a flexible linker and designated AN-VN or AN-VC, respectively. To determine whether BiFC can efficiently detect the N-N interactions in living cells, cells were cotransfected with AN-VN and AN-VC and examined for fluorescence. At 16 h posttransfection, we found that fluorescence, representing the N-N interaction, was distributed throughout the cytoplasm and in the nucleoli (Fig. 7B, panel d). To investigate the specificity of the BiFC assay, the α-tubulin gene then was amplified from MARC-145 cells and ligated to the N terminus of VN or VC, and the resulting constructs were designated Tubulin-VN and Tubulin-VC, respectively. The AN-VN/Tubulin-VC and AN-VC/Tubulin-VN pairs were employed as negative controls, and when transfected into living cells neither produced any positive BiFC signals (Fig. 7B, panels b and c), which confirmed the feasibility of the BiFC assay in studying the N-N interactions.

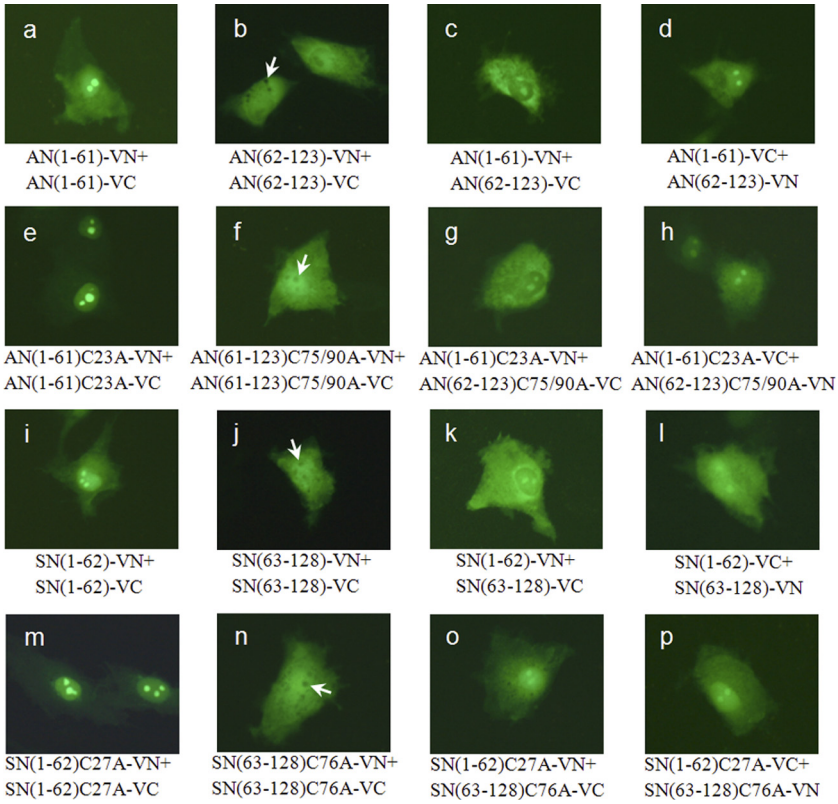

FIG 8 BiFC analysis of truncated N proteins. Full-length N proteins with or without cysteine mutations were split between amino acid residues 61 and 62 for APRRS or between 62 and 63 for SHE. The resulting halves were ligated to VN or VC, MARC-145 cells were transfected, and fluorescent signals were visualized. The arrows indicate the nucleoli with no fluorescence.

We next extended the BiFC approach to investigate potential interactions between N proteins for both genotypes of PRRSV. First, to ascertain whether the cysteines affect the N-N interactions, ANC23A-VN/ANC23A-VC and ANC23/75/90A-VN/ANC23/75/90A-VC pairs, in which full-length N proteins of APRRS contain the C23A and C23/75/90A mutations, respectively, were generated by the strategy described above. Cells cotransfected with these pairs gave rise to fluorescent signals similar to those for AN-VN/AN-VC (Fig. 7B, panels e and f). Likewise, we generated BiFC constructs fused with the full-length wild-type, C27A, and C27/76A N proteins of type I SHE and found that the coexpression of these BiFC combinations resulted in strong fluorescent signals (Fig. 7B, panels g to i). The fluorescence produced by these BiFC pairs demonstrated that there is an intermolecular interaction between the N proteins regardless of the cysteine mutations in either genotype of PRRSV. This finding is in agreement with previously reported data obtained from both well-established *in vitro* glutathione *S*-transferase (GST) pulldown and *in vivo* mammalian two-hybrid assays (59). We attempted to further probe the interactions between N proteins. To this end, we split the N protein of APRRS (as shown in Fig. 2A), and the N-terminal 61 and C-terminal 62 amino acids were fused to VN or VC, generating AN(1-61)-VN/AN(1-61)-VC and AN(62-123)-VN/AN(62-123)-VC, respectively. The coexpression of the N or C termini of N proteins in the BiFC pairs described above produced good fluorescence complementation (Fig. 8a and b), indicating that both the N and C termini of N form intermolecular interactions. It is noteworthy that obvious fluorescence was detected after cotransfection with the AN(1-61)-VN/AN(62-123)-VC or AN(1-61)-VC/AN(62-123)-VN combination in which only the N-terminal and C-terminal halves of the N protein were coexpressed in cells (Fig. 8c and d). This finding was suggestive of a heterodimeric or intramolecular interaction between the N- and C-terminal regions of N proteins. The same observation was made when the cysteine residues were removed from the truncated N proteins (Fig. 8e to h). Moreover, we conducted similar experiments for the type I SHE protein, for which we cleaved the N protein between amino acids 62 and 63 according to the sequence alignment in Fig. 2A, and we found fluorescent intensities similar to those of the truncated N proteins of type II APRRS (Fig. 8i to p). Taken together, these data obtained from BiFC analysis in living cells led us to conclude that interactions occurred among the N or C termini of N proteins and also between the N- and C-terminal regions of N proteins, either with or without cysteine residues, for both type II and type I PRRSV.

In addition, we observed an interesting phenomenon in which the nucleoli revealed no fluorescence in Fig. 8b, f, j and n, which can be explained by the fact that the N-terminally truncated N proteins lack the nucleolar location signal (NoLS) sequences (42, 43). The presence of fluorescence in the nucleoli in Fig. 7B and 8 indicates N-N interactions in these areas, implying that the NoLS sequences in the N terminus are able to guide the binary full-length or truncated N protein complexes to migrate from the cytoplasm into the nucleoli.

DISCUSSION

In this paper, we report that the ORF7 3′UTR or ORF7 of type I PRRSV can be swapped into the type II PRRSV genomic background in spite of the low intergenotypic sequence identity, and that the N protein cysteine residues are not essential for the infectivity of either PRRSV genotype. These chimeric viruses were genetically stable and their growth properties similar to those of the parental viruses, with the exception of vA-SHE73′, in which ORF6 and ORF7 were separated. The growth rate and sgmRNA level of vA-SHE73′ were found to be significantly decreased, whereas vA-OSHE73′ showed only proportionately reduced sgmRNAs compared to that of the wild type. The TRS-flanking sequences have been previously reported to play a role in regulating nidoviral transcription (40). Whether our chimeric manipulations altered the local flanking sequence of TRS-B and its secondary structure, thereby greatly affecting the viral transcription or replication, is a focus of our ongoing study. It has been reported that a stretch of 34 nucleotides within ORF7 of LV, the prototypic type I PRRSV, is essential for RNA replication, and a 7-base core sequence within this stretch is engaged in a kissing-loop interaction with a stem-loop structure located in the 3′UTR (50, 51). The 34-nucleotide stretch in ORF7 is well conserved between the genotypes. Our chimeric virus vA-OSHE7, in which ORF7 of type I was forced to replace its counterpart in type II PRRSV in an exact ORF-for-ORF substitution, demonstrated that the heterologous ORF7 of type I is compatible with the type II 3′UTR and does not disrupt the kissing-loop interaction.

The fact that the heterologous N gene of type I is functional in the type II PRRSV genomic background lays the foundation for further investigations of the structure-function relationships of the N protein. The conserved domains or critical amino acid residues of N proteins from the two genotypes may share the same functions, such as the RNA-binding domains, nuclear localization signal sequences, phosphorylation sites, and conformation-determining domains. Comparative analysis suggested to us that Cys90 of the type II PRRSV N protein is nonexistent in the type I isolates and thus could be irrelevant to N functions. Cysteine-to-serine mutational analysis had previously shown that Cys90 and Cys23, but not Cys75, are essential for virus infectivity (31). It was further speculated that Cys90 engages in a possible disulfide linkage with another type II PRRSV structural protein. For example, the type II PRRSV E protein contains two cysteines at positions 49 and 54, while type I isolates contain only a single cysteine at position 51 (56, 60). However, data from a previous study disproved the hypothesis that the E and N proteins interact through their cysteine residues (32). The functional significance of Cys90 in type II N proteins is still undefined. In the present study, the Cys90-to-alanine mutation in combination with the chimera results unambiguously demonstrated that this cysteine is nonessential for virus infectivity, suggesting either that Cys90 does not mediate the covalent interactions between N and other structural proteins in type II PRRSV or that Cys90 is involved but not essential.

Furthermore, one of the most remarkable findings from our genetic studies was that all of the cysteine residues of the N protein could be knocked out for both genotypes of PRRSV, which challenges previous reports that Cys23-mediated disulfide-linked N dimerization is essential for virus infectivity (31, 59). To investigate the biological significance of the N protein cysteines and resolve this apparently conflicting data, we repeated the biochemical work to mimic that conducted in the previous study (59) for types II and I PRRSV. Although we demonstrated that Cys23 in type II or Cys27 in type I N participated in disulfide-linked homodimerization in cell lysates exposed to an oxidizing environment, a portion of the N proteins in extracellular virions treated with NEM still formed homodimers under nonreducing conditions, which is suggestive of disulfide bond formation between N proteins in virions. The application of different virus purification procedures did not produce direct evidence from virions to reject the result described above. These observations were fully consistent with the previous findings (59), supporting the notion that disulfide bonds participate in virus particle assembly and the stabilization of the capsid structure as reported for other viruses (23, 29, 33, 41, 48, 52). However, it was surprising that the mutant viruses that completely prevented disulfide-linked N dimerization in virus particles, such as vAN-C23A and vSN-C27A (Fig. 6A and B), still showed growth properties comparable to those of parental viruses (Fig. 3B and C and 4B and C). The likely explanation for these observations is that the cysteine-mediated disulfide linkages in N dimers have subtle effects on virion stability, or that the noncovalent interactions between N proteins are more important for N dimerization during virus particle assembly, and it is the noncovalent interactions that position the cysteines for disulfide formation, which in turn reinforces the noncovalent interactions. It is noteworthy that both monomers and dimers of N protein were present in extracellular virions (Fig. 6C), suggesting that not all of the N proteins in virions were dimerized. Thus, it remains possible that disulfide-linked N dimers detected from purified virions were actually an artifact of lysis, as the purification procedures may not have produced highly purified intact virions. In addition, it is also likely that the penetration of the alkylating agent NEM into virions was less effective than that in living cells. The compact structure of the virion may hamper the effective modification of cysteine thiols in the N protein. Moreover, since other members of the family *Arteriviridae*, such as EAV and SHFV, completely lack cysteines in the N protein (10, 15), the virus assembly mechanism would be expected to be the same among the arteriviruses; however, this hypothesis requires further investigation.

In the current study, the successful replacement of cysteine with alanine at position 23 or 90 in the type II N protein led us to speculate about the reasons for the difference in outcome from the similar cysteine-to-serine mutagenesis in previous work (31). The replacement of target amino acids with alanine removes the side chains beyond the β-carbon without changing the main-chain conformation or imposing extreme electrostatic or steric effects (9). The cysteine-to-alanine mutation conserves the hydrophobic character, while the cysteine-to-serine replacement results in a more hydrophilic side chain and a relatively small change of size (30, 54). The crystal structure of a partial type II PRRSV N protein indicated that the C-terminal half exists as a dimer, and the rather hydrophobic β sheet floors make up the internal surface of the shell (11). Cys90 is located only on the β1 strand (Fig. 2A), and Cys23 is presumed to be located in the interior of the nucleocapsid based on the proposed model (11). Therefore, while it cannot be ascertained at present, the substitution of the more hydrophilic serine residue may affect the structural stability of the N protein; for example, the more polar hydroxyl group of serine may change the positioning of other amino acids via hydrogen bond formation. However, we still do not know how to explain properly our

successful rescue of pAN-C23S, which was lethal in a previous study (31). The previously reported lethal effect of C23S may be a strain-specific observation. The rescue of pAN-C23S, albeit with a retarded growth rate, clearly demonstrated that Cys23 is nonessential for virus infectivity.

The fact that disulfide-linked N dimers are present in the mature virions seems to be contradictory to our genetic evidence, which indicated that all of the cysteines can be knocked out without effect. Thus, the further study of specific N-N interactions can greatly contribute to our understanding of N protein dimerization and virus particle assembly. In this study, we used a BiFC assay to investigate the interactions between N proteins in living cells. The advantage of this method is its capacity to directly visualize, under physiological conditions, weak or transient protein-protein interactions that cannot be detected by traditional biochemical techniques. Although developed only recently, this assay has been widely employed to investigate viral protein-protein interactions (2, 3, 5, 6, 20, 24, 26, 64). Previous reports using the GST pulldown assay have shown that amino acids 30 to 37 are essential for N-N interactions (59). The crystal structure of the C-terminal part of the type II PRRSV N protein shows a tight dimer, indicating the existence of interactions between the C-terminal regions (11). Here, we used BiFC to demonstrate not only intermolecular interactions between the full-length N proteins but also interactions among the N or C termini, as well as possible inter- or intramolecular interactions between the N- and C-terminal regions of N proteins, either with or without cysteine residues, implying an important role of noncovalent interactions in particle assembly. Furthermore, the nucleolar localization of N-N interactions in living cells was illustrated, which should be helpful in furthering our knowledge of the characteristics and functionality of the N protein.

Taken together, our results show that the nucleocapsid proteins from two genotypes of PRRSV are exchangeable, and that none of the type II or I N protein cysteines is essential for virus infectivity. We have once again confirmed that disulfide-linked N dimers are present in extracellular virions and also defined the interacting domains of the N proteins by using a BiFC assay. These findings suggest that the disulfide linkages mediating N dimerization are not required during PRRSV particle formation, which will be of great significance in further understanding the role of N dimerization and the mechanism of arterivirus virion assembly.

ACKNOWLEDGMENTS

We thank the members of the Yuan laboratory for helpful discussions and suggestions throughout the course of this study. We also thank Judith M. Phillips and Zachary Zalinger in the Weiss laboratory at the University of Pennsylvania for help in editing the manuscript.

This work was funded by the China Natural Science Foundation (no. 30972204), the EU Seventh Framework Program (no. 245141), and the Shanghai Municipal Science and Technology Special Programs (no. 083219n1300 and 08ZR1422800) to S.Y.

REFERENCES

1. **Allende R, et al.** 1999. North American and European porcine reproductive and respiratory syndrome viruses differ in non-structural protein coding regions. J. Gen. Virol. **80**:307–315.
2. **Aparicio F, Sanchez-Navarro JA, Pallas V.** 2006. In vitro and in vivo mapping of the Prunus necrotic ringspot virus coat protein C-terminal dimerization domain by bimolecular fluorescence complementation. J. Gen. Virol. **87**:1745–1750.
3. **Atanasiu D, et al.** 2007. Bimolecular complementation reveals that glycoproteins gB and gH/gL of herpes simplex virus interact with each other during cell fusion. Proc. Natl. Acad. Sci. U. S. A. **104**:18718–18723.
4. **Benfield DA, et al.** 1992. Characterization of swine infertility and respiratory syndrome (SIRS) virus (isolate ATCC VR-2332). J. Vet. Diagn. Investig. **4**:127–133.
5. **Boyko V, et al.** 2006. Coassembly and complementation of Gag proteins from HIV-1 and HIV-2, two distinct human pathogens. Mol. Cell **23**:281–287.
6. **Buck CB, et al.** 2008. Arrangement of L2 within the papillomavirus capsid. J. Virol. **82**:5190–5197.
7. **Cavanagh D.** 1997. Nidovirales: a new order comprising Coronaviridae and Arteriviridae. Arch. Virol. **142**:629–633.
8. **Cowley JA, Dimmock CM, Spann KM, Walker PJ.** 2000. Gill-associated virus of Penaeus monodon prawns: an invertebrate virus with ORF1a and ORF1b genes related to arteri- and coronaviruses. J. Gen. Virol. **81**:1473–1484.
9. **Cunningham BC, Wells JA.** 1989. High-resolution epitope mapping of hGH-receptor interactions by alanine-scanning mutagenesis. Science **244**:1081–1085.
10. **den Boon JA, et al.** 1991. Equine arteritis virus is not a togavirus but belongs to the coronaviruslike superfamily. J. Virol. **65**:2910–2920.
11. **Doan DN, Dokland T.** 2003. Structure of the nucleocapsid protein of porcine reproductive and respiratory syndrome virus. Structure **11**:1445–1451.
12. **Dokland T.** 2010. The structural biology of PRRSV. Virus Res. **154**:86–97.
13. **Firth AE, et al.** 2011. Discovery of a small arterivirus gene that overlaps the GP5 coding sequence and is important for virus production. J. Gen. Virol. **92**:1097–1106.
14. **Forsberg R.** 2005. Divergence time of porcine reproductive and respiratory syndrome virus subtypes. Mol. Biol. Evol. **22**:2131–2134.
15. **Godeny EK, Zeng L, Smith SL, Brinton MA.** 1995. Molecular characterization of the 3′ terminus of the simian hemorrhagic fever virus genome. J. Virol. **69**:2679–2683.
16. **Gorbalenya AE, Enjuanes L, Ziebuhr J, Snijder EJ.** 2006. Nidovirales: evolving the largest RNA virus genome. Virus Res. **117**:17–37.
17. **Gouet P, Courcelle E, Stuart DI, Metoz F.** 1999. ESPript: analysis of multiple sequence alignments in PostScript. Bioinformatics **15**:305–308.
18. **Hanada K, Suzuki Y, Nakane T, Hirose O, Gojobori T.** 2005. The origin and evolution of porcine reproductive and respiratory syndrome viruses. Mol. Biol. Evol. **22**:1024–1031.
19. **Heckman KL, Pease LR.** 2007. Gene splicing and mutagenesis by PCR-driven overlap extension. Nat. Protoc. **2**:924–932.
20. **Hemerka JN, et al.** 2009. Detection and characterization of influenza A virus PA-PB2 interaction through a bimolecular fluorescence complementation assay. J. Virol. **83**:3944–3955.
21. **Hu CD, Chinenov Y, Kerppola TK.** 2002. Visualization of interactions among bZIP and Rel family proteins in living cells using bimolecular fluorescence complementation. Mol. Cell **9**:789–798.
22. **Hu CD, Kerppola TK.** 2003. Simultaneous visualization of multiple protein interactions in living cells using multicolor fluorescence complementation analysis. Nat. Biotechnol. **21**:539–545.
23. **Jeng KS, Hu CP, Chang CM.** 1991. Differential formation of disulfide linkages in the core antigen of extracellular and intracellular hepatitis B virus core particles. J. Virol. **65**:3924–3927.
24. **Jin J, et al.** 2007. Distinct intracellular trafficking of equine infectious anemia virus and human immunodeficiency virus type 1 Gag during viral assembly and budding revealed by bimolecular fluorescence complementation assays. J. Virol. **81**:11226–11235.
25. **Johnson CR, Griggs TF, Gnanandarajah J, Murtaugh MP.** 2011. Novel structural protein in porcine reproductive and respiratory syndrome virus encoded by an alternative ORF5 present in all arteriviruses. J. Gen. Virol. **92**:1107–1116.
26. **Kenney SP, Lochmann TL, Schmid CL, Parent LJ.** 2008. Intermolecular interactions between retroviral Gag proteins in the nucleus. J. Virol. **82**:683–691.
27. **Kerppola TK.** 2006. Complementary methods for studies of protein interactions in living cells. Nat. Methods **3**:969–971.
28. **Kuo LL, Harty JT, Erickson L, Palmer GA, Plagemann PG.** 1991. A nested set of eight RNAs is formed in macrophages infected with lactate dehydrogenase-elevating virus. J. Virol. **65**:5118–5123.
29. **Kushima Y, Wakita T, Hijikata M.** 2010. A disulfide-bonded dimer of the core protein of hepatitis C virus is important for virus-like particle production. J. Virol. **84**:9118–9127.

30. **Kyte J, Doolittle RF.** 1982. A simple method for displaying the hydropathic character of a protein. J. Mol. Biol. **157**:105–132.
31. **Lee C, Calvert JG, Welch SK, Yoo D.** 2005. A DNA-launched reverse genetics system for porcine reproductive and respiratory syndrome virus reveals that homodimerization of the nucleocapsid protein is essential for virus infectivity. Virology **331**:47–62.
32. **Lee C, Yoo D.** 2005. Cysteine residues of the porcine reproductive and respiratory syndrome virus small envelope protein are non-essential for virus infectivity. J. Gen. Virol. **86**:3091–3096.
33. **Li M, Beard P, Estes PA, Lyon MK, Garcea RL.** 1998. Intercapsomeric disulfide bonds in papillomavirus assembly and disassembly. J. Virol. **72**: 2160–2167.
34. **Mateu E, Diaz I.** 2008. The challenge of PRRS immunology. Vet. J. **177**:345–351.
35. **Meulenberg JJ.** 2000. PRRSV, the virus. Vet. Res. **31**:11–21.
36. **Meulenberg JJ, et al.** 1993. Lelystad virus, the causative agent of porcine epidemic abortion and respiratory syndrome (PEARS), is related to LDV and EAV. Virology **192**:62–72.
37. **Meulenberg JJ, et al.** 1998. Localization and fine mapping of antigenic sites on the nucleocapsid protein N of porcine reproductive and respiratory syndrome virus with monoclonal antibodies. Virology **252**:106–114.
38. **Nagai T, et al.** 2002. A variant of yellow fluorescent protein with fast and efficient maturation for cell-biological applications. Nat. Biotechnol. **20**: 87–90.
39. **Nelsen CJ, Murtaugh MP, Faaberg KS.** 1999. Porcine reproductive and respiratory syndrome virus comparison: divergent evolution on two continents. J. Virol. **73**:270–280.
40. **Pasternak AO, Spaan WJ, Snijder EJ.** 2006. Nidovirus transcription: how to make sense? J. Gen. Virol. **87**:1403–1421.
41. **Pornillos O, Ganser-Pornillos BK, Banumathi S, Hua Y, Yeager M.** 2010. Disulfide bond stabilization of the hexameric capsomer of human immunodeficiency virus. J. Mol. Biol. **401**:985–995.
42. **Rowland RR, Kervin R, Kuckleburg C, Sperlich A, Benfield DA.** 1999. The localization of porcine reproductive and respiratory syndrome virus nucleocapsid protein to the nucleolus of infected cells and identification of a potential nucleolar localization signal sequence. Virus Res. **64**:1–12.
43. **Rowland RR, Yoo D.** 2003. Nucleolar-cytoplasmic shuttling of PRRSV nucleocapsid protein: a simple case of molecular mimicry or the complex regulation by nuclear import, nucleolar localization and nuclear export signal sequences. Virus Res. **95**:23–33.
44. **Shimozono S, Miyawaki A.** 2008. Engineering FRET constructs using CFP and YFP, p. 381–393. *In* Kevin FS (ed.), Methods in cell biology, vol. 85. Academic Press, New York, NY.
45. **Shyu YJ, Hu CD.** 2008. Fluorescence complementation: an emerging tool for biological research. Trends Biotechnol. **26**:622–630.
46. **Shyu YJ, Liu H, Deng X, Hu CD.** 2006. Identification of new fluorescent protein fragments for bimolecular fluorescence complementation analysis under physiological conditions. Biotechniques **40**:61–66.
47. **Snijder EJ, Meulenberg JJ.** 1998. The molecular biology of arteriviruses. J. Gen. Virol. **79**:961–979.
48. **Szczepaniak R, et al.** 2011. Disulfide bond formation contributes to herpes simplex virus capsid stability and retention of pentons. J. Virol. **85**:8625–8634.
49. **Tian D, Zheng H, Zhang R, Zhuang J, Yuan S.** 2011. Chimeric porcine reproductive and respiratory syndrome viruses reveal full function of genotype 1 envelope proteins in the backbone of genotype 2. Virology **412**: 1–8.
50. **Verheije MH, Kroese MV, Rottier PJ, Meulenberg JJ.** 2001. Viable porcine arteriviruses with deletions proximal to the 3′ end of the genome. J. Gen. Virol. **82**:2607–2614.
51. **Verheije MH, Olsthoorn RC, Kroese MV, Rottier PJ, Meulenberg JJ.** 2002. Kissing interaction between 3′ noncoding and coding sequences is essential for porcine arterivirus RNA replication. J. Virol. **76**:1521–1526.
52. **Wang CH, et al.** 2010. Roles of cysteines Cys115 and Cys201 in the assembly and thermostability of grouper betanodavirus particles. Virus Genes **41**:73–80.
53. **Wensvoort G, et al.** 1991. Mystery swine disease in The Netherlands: the isolation of Lelystad virus. Vet. Q. **13**:121–130.
54. **Wolfenden R, Andersson L, Cullis PM, Southgate CC.** 1981. Affinities of amino acid side chains for solvent water. Biochemistry **20**:849–855.
55. **Wootton S, Koljesar G, Yang L, Yoon KJ, Yoo D.** 2001. Antigenic importance of the carboxy-terminal beta-strand of the porcine reproductive and respiratory syndrome virus nucleocapsid protein. Clin. Diagn. Lab. Immunol. **8**:598–603.
56. **Wootton S, Yoo D, Rogan D.** 2000. Full-length sequence of a Canadian porcine reproductive and respiratory syndrome virus (PRRSV) isolate. Arch. Virol. **145**:2297–2323.
57. **Wootton SK, Nelson EA, Yoo D.** 1998. Antigenic structure of the nucleocapsid protein of porcine reproductive and respiratory syndrome virus. Clin. Diagn. Lab. Immunol. **5**:773–779.
58. **Wootton SK, Rowland RR, Yoo D.** 2002. Phosphorylation of the porcine reproductive and respiratory syndrome virus nucleocapsid protein. J. Virol. **76**:10569–10576.
59. **Wootton SK, Yoo D.** 2003. Homo-oligomerization of the porcine reproductive and respiratory syndrome virus nucleocapsid protein and the role of disulfide linkages. J. Virol. **77**:4546–4557.
60. **Wu WH, et al.** 2001. A 10-kDa structural protein of porcine reproductive and respiratory syndrome virus encoded by ORF2b. Virology **287**:183–191.
61. **Wu WH, et al.** 2005. The 2b protein as a minor structural component of PRRSV. Virus Res. **114**:177–181.
62. **Yoo D, Wootton SK, Li G, Song C, Rowland RR.** 2003. Colocalization and interaction of the porcine arterivirus nucleocapsid protein with the small nucleolar RNA-associated protein fibrillarin. J. Virol. **77**:12173–12183.
63. **Yuan S, Wei Z.** 2008. Construction of infectious cDNA clones of PRRSV: separation of coding regions for nonstructural and structural proteins. Sci. China **51**:271–279.
64. **Zamoto-Niikura A, Terasaki K, Ikegami T, Peters CJ, Makino S.** 2009. Rift valley fever virus L protein forms a biologically active oligomer. J. Virol. **83**:12779–12789.